

First Measurement of Potential in the Core Region of the Madison Symmetric Torus Reversed Field Pinch

CONNOR Kenneth*, SHAH Uday, LEI Jianxin, DEMERS Diane,
SCHOCH Paul, CROWLEY Thomas, FOREST Cary¹, ANDERSON Jay¹,
CRAIG Darren^b, PRAGER Stewart^b and the MST Team^b
Rensselaer Polytechnic Institute, Troy, NY 12180-3590, USA
¹*University of Wisconsin, Madison, WI, 53706-1390, USA*

(Received: 5 December 2000 / Accepted: 27 September 2001)

Abstract

Determination of the plasma potential in the core of the Madison Symmetric Torus (MST) Reversed Field Pinch (RFP) is one of the primary purposes of the MST Heavy Ion Beam Probe (HIBP). In particular, the relationship between the equilibrium electric field and plasma rotation and transport will be investigated. Preliminary measurements inside the core indicate that the plasma potential Φ_p is positive and in the range of 0.5 kV to 2.5 kV for standard discharges (including the range of observed potentials and possible errors). This is the first such measurement in the core of an RFP with moderate temperature and density. Because an RFP magnetic field is produced by plasma currents, initial experiments have emphasized finding Φ_p at locations known to be in the core of standard discharges, even though the magnetic field and, thus, the locations themselves are not fully known. The sensitivity of the beam ion orbits to the current profile is being exploited by using the HIBP signals to provide a constraint on the magnetic equilibrium model and thereby help determine the current profile. A simple density scaling experiment has been performed showing a significant decrease in Φ_p with increasing density. The intriguing, though preliminary results from this and other experiments point to a significant role for Φ_p measurements in an RFP.

Keywords:

plasma potential, Heavy Ion Beam Probe, HIBP, reversed field pinch, Madison Symmetric Torus, MST

1. Introduction

Heavy Ion Beam Probes (HIBP) [1] measure a variety of plasma parameters in magnetically confined plasmas, including the electrostatic potential profile $\Phi(r)$, potential fluctuations $\tilde{\Phi}(r)$ and electron density fluctuations $\tilde{n}_e(r)$. For the first time, an HIBP system has been installed on a reversed field pinch (RFP), the Madison Symmetric Torus (MST), to investigate the importance of the electrostatic potential profile and various fluctuations on confinement and particle transport in the core of an RFP [2]. Unique to the MST-

HIBP system, the equilibrium magnetic field $\vec{B}(\vec{r})$ can also be investigated. The HIBP has produced detectable signal for only a few months, producing some intriguing, though preliminary, data of all types that strongly suggest a significant impact will be made on RFP research.

In a beam probe diagnostic system, singly charged (primary) ions produced by an ion accelerator are guided into the plasma by a series of electrostatic sweep plates in the primary beamline (see Fig. 1 for the general

*Corresponding author's e-mail: connor@rpi.edu

outline of the MST-HIBP). As the primary beam passes through the plasma, doubly charged (secondary) ions are created by collisions with plasma electrons. These ions are separated from the primary beam by the confining magnetic field and some pass out of the plasma vacuum chamber into the secondary beamline, where a second series of sweep plates guides them to the detector (an electrostatic energy analyzer). A fraction of the secondary ions pass through a small aperture into the detector. These ions originate in a small piece of the injected primary beam (sample volume). Information on the electron density, electric potential and magnetic field is contained in the detected secondary ion intensity, energy and toroidal deflection, respectively.

The implementation the MST-HIBP had to deal with several design issues, all of which affect potential measurements. First, the MST vacuum vessel has very small ports to minimize magnetic field errors. For ease of operation and to maximize plasma coverage, an HIBP generally works best with the largest available ports. Second, the UV and plasma particle flux levels through the MST diagnostic ports are very high. Such intense flux impedes the operation of the many HIBP electric field structures (sweep plates, accelerator and energy analyzer) and produces potentially high levels of noise in the detected signal. Third, the confining magnetic field of an RFP is largely generated by plasma currents and thus is only partly known. Full knowledge of magnetic field is necessary to accurately determine the measurement location (sample volume). Finally, *in situ* calibration of the MST-HIBP is difficult because it is not possible to either direct the primary beam into the analyzer, as was done most effectively on bumpy tori, or the detect secondaries when the potential is known to be small or when there is little or no plasma, as on stellarators [1].

In section 2, we discuss how the HIBP is presently being used to measure potential on MST. The methodology by which the HIBP is being used to help improve the equilibrium magnetic field model is presented in section 3. The first systematic potential measurement experiment on MST, in which plasma operating conditions are held roughly constant while density is varied from shot-to-shot, is described in section 4. Future plans are covered in section 5.

2. HIBP Potential Measurements on MST

The basic methodology for making a potential measurement is quite simple. Initial conditions for probing ion trajectories are determined that have a

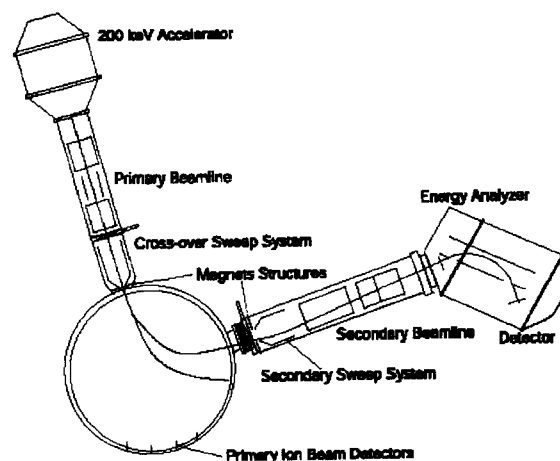


Fig. 1 A schematic view of the MST-HIBP

sample point in the core plasma and reach the entrance aperture of the energy analyzer. Such a trajectory is shown generically in Fig. 1. To reach the desired plasma location, the accelerator and analyzer voltages, as well as the voltages on the many sets of sweep plates must be specified. Once a set of voltages has been determined that produces detectable signal (see Fig. 5 of [3]), all voltages are set accordingly. In addition, triangular AC voltages are added to the DC voltages to cover a range of conditions around those predicted from trajectory calculations, since the B field model used to determine the trajectories is not exact. To measure the potential at a single location, the sweep voltages are fixed at the values found to produce signal at some point in the discharge. This does not however, guarantee that signal will consistently be obtained throughout a discharge.

The detected ions follow a trajectory like that of Fig. 1, ending on ion current detection plates. These plates are split vertically and horizontally so that four separate currents are monitored. The currents on the top two plates are summed to produce i_{upper} while the bottom two plates sum to i_{lower} . The energy of the secondary ion leaving the plasma differs from that of the primary ion by the change in potential energy $(q_s - q_p)\Phi_p$. Thus, to determine potential, we use a Proca and Green type energy analyzer and the following relationship [4]

$$\Phi_p = \frac{+q_s V_{AN}}{q_s - q_p} \left(G(\theta) + F_{HIBP}(\theta) \frac{\Delta i}{i} \right) - \frac{q_p V_{AC}}{q_s - q_p}$$

where $G(\theta)$ and $F_{\text{HIBP}}(\theta)^*$ are geometric functions of the analyzer entrance angle θ , $\Delta i = i_{\text{upper}} - i_{\text{lower}}$, $i = i_{\text{upper}} + i_{\text{lower}}$, q_s and q_p are the charges of the secondary and primary ions, V_{AN} is the analyzer voltage and V_{AC} is the accelerator voltage.

The measurement of G is described elsewhere [3,4]. At present, there remains an instrumental uncertainty in G the order of 1%. The impact of this uncertainty is described in section 4. A similar uncertainty in F_{HIBP} is much less important because the F_{HIBP} term is much smaller. Measurement errors also occur due to inaccuracies in the monitoring of the analyzer and accelerator voltages. Errors in G of this scale will dominate all other errors. Experiments are planned to measure G more accurately both with and without plasma.

3. Using the HIBP to Improve the MST Equilibrium Model

The orbits of the beam ions are very sensitive to details of the current profile in the RFP. This is easily seen by observing any of the detector plate signals during a sawtooth oscillation. This sensitivity can be exploited by using the HIBP signals (when observed) to provide a constraint on the magnetic equilibrium and thereby help determine the current profile. The technique used is as follows. When a signal is detected, several pieces of information are known. First, the injector and detector settings at a given instant in time can be mapped onto the injection velocity and a detected ion velocity. The observation of signal implies that the primary and secondary trajectories overlap at some point in the plasma, and that at that point in the orbit the beam velocities must match. This information is incorporated into the equilibrium reconstruction code by minimizing a cost function related to the distance of closest approach and the difference in velocities at that point. A non-linear search algorithm is used to simultaneously find the best fit to this information together with other magnetic diagnostics.

The injection velocity is relatively easy to determine from the accelerator voltage and the sweep angles produced by the primary beamline sweep plates. No knowledge of the confining magnetic field is required. The detected ion velocity should be more difficult to determine because it depends on the magnetic field. However, because the first set of sweep

plates in the secondary beamline is made inoperable by intense UV flux [4,5], the possible angular range of the secondary ions is so limited that a small range of possible values can be found.

Figure 2 shows how the improvements in the equilibrium code are manifested for the measurement conditions used to obtain the data presented below. The evolution of the field model over the last few years is found in plot (a), while the impact on the measurement locations (sample volumes) and trajectories are shown in (b)–(d). Only a small number of cases have been addressed, so the results shown only demonstrate that this process should be able to lead to an improved equilibrium model, as incorporation of information from other diagnostics have generated the large changes of the most recent field model achieved without an HIBP contribution. However, it is very encouraging to realize additional HIBP capabilities while also improving our measurements by better determination of sample locations. Such an approach could be applied to other confinement schemes with a large contribution to the confining field from plasma currents, such as compact stellarators.

4. Density Scan

Figure 3 shows HIBP data[#] taken from 10–30ms during a standard 360 kA discharge with a density of 10^{13} cm^{-3} . The top trace is the potential determined as described above. The next four traces are the currents on the four detector plates. The first feature to note in all of the detector signals is the UV burst produced by sawteeth at about 11, 19 and 27 ms. The UV creates secondary electron current on the plates that looks like secondary ion signal. However, the UV more or less uniformly floods the entire analyzer and thus produces very similar signals on all four plates. The location where the secondary ions impact the detector plates changes with time due to changes in potential and/or magnetic field and, thus, these signals are rarely the same on each plate, as described in section 3. It is difficult to measure potential during sawteeth, primarily because the background noise level is so high. Thus, to emphasize reliable, representative data for each shot, time periods that are at least one millisecond from the beginning or end of a sawtooth are processed. These

* The letter F plays a key role in both RFP and HIBP notation. $F = B_\phi(a)/\langle B_\phi \rangle$ is the RFP reversal parameter. These two parameters will be distinguished by subscripts in this paper.

[#] The measurement location for this and all other data presented in this paper is about $r/a = 0.5$, as shown in Fig. 2 (b). Recall that there is some uncertainty in this location, but the measurement is definitely in the core plasma. The probing ion for all cases was 70.5 keV sodium.

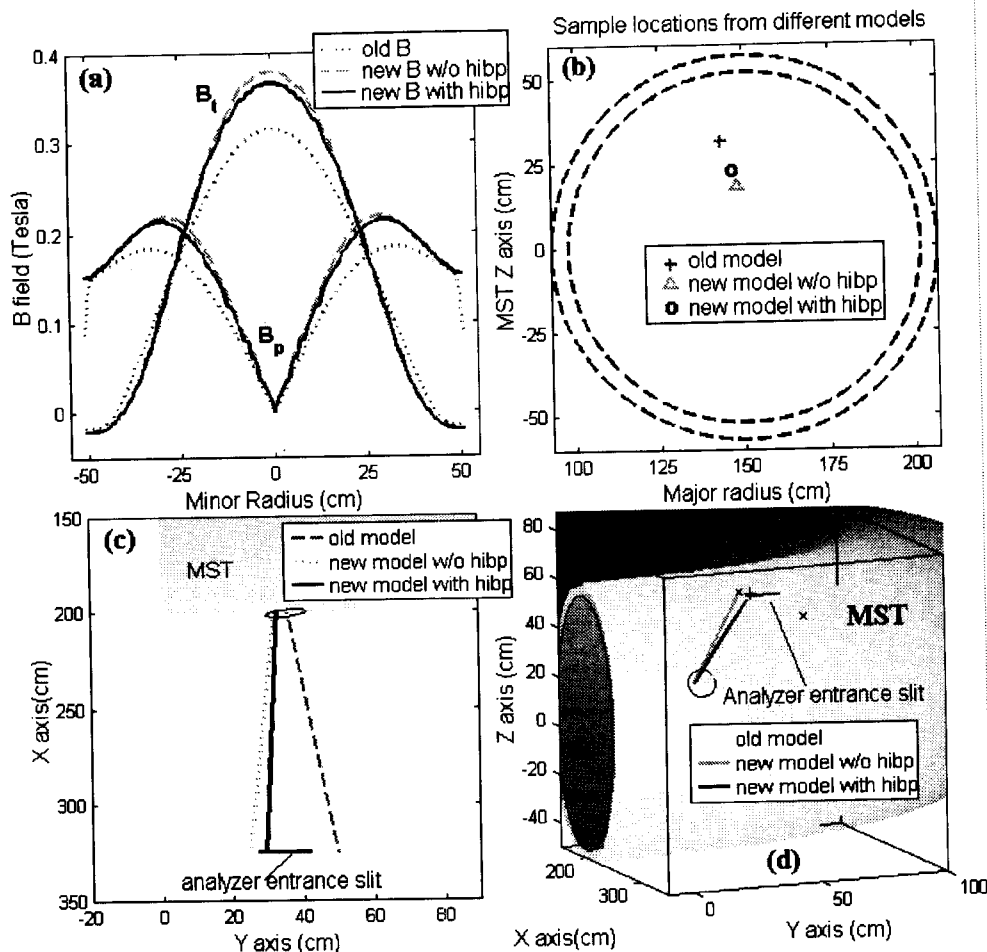


Fig. 2 Comparison of the three magnetic field models used to develop the HIBP (old model, new model without HIBP data, new model with HIBP data): (a) toroidal and poloidal field components; (b) sample locations; (c) secondary trajectories after they leave MST chamber (top view); (d) 3-D view of secondary trajectories.

sawtooth-free time periods can be as long as 13 ms. Typically, the potential rises after the sawtooth crash, reaches a maximum value (which is not always very distinct) and then decreases before the onset of the next sawtooth. Between sawteeth, the potential can vary by hundreds of volts but does not appear to undergo any large jumps.

The simplest approach to identifying any broad trends in the dependence of the potential on density is to take a large number of shots over a range of densities and record all results. Essentially all reliable potential values found in a sequence of 50 shots are shown as a scatter plot in Fig. 4. For these shots the plasma current was about 360kA and the reversal parameter F_{RFP} was about -0.23 while the pinch parameter Θ was about 1.75. The plasma configuration was most sensitive to the plasma current, so operating conditions were set to

achieve the desired current to within a few percent. The potential was much less sensitive to changes in F_{RFP} and Θ . A general decline in the potential as the density increases is apparent. To highlight this dependence, the average of all potentials observed at each density is also shown, as is a curve fit to the average points. In general, the temperature decreases in a similar manner with density. However, this simple exercise was only meant to motivate further inquiry, not to identify a specific scaling law. Recall also that the largest uncertainty in the potential measurement is the geometric gain term G . For the data shown, G was assumed to be 3.00 while F_{HIBP} was 0.041 (the best presently available values for these parameters). If, as we suspect could be the case, G were a bit more than 1% smaller, the error in the potentials should be about 900 V for an analyzer voltage of 12 kV. This error would equally reduce all measured

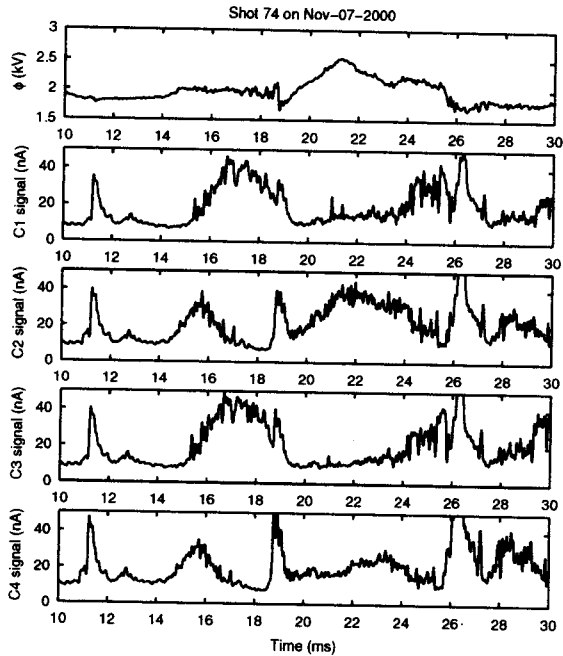


Fig. 3 **Shot 74 (7 November)** The signals shown are, in order from top to bottom: potential; detected signal on upper left plate; detected signal on upper right plate; detected signal on lower left plate; detected signal on lower right plate. Measurements are made at $r/a = 0.5$.

potentials. The average of these reduced potentials would fit quite a different density dependence ($n_e^{-0.6}$). All other sources of error that could affect the relationship between density and potential are much smaller. For example, a small amount of ion energy loss can occur due to multiple small angle Coulomb collisions. At the densities considered here, this will not be significant [1].

The purpose of this experiment was primarily to see if a systematic change in potential occurred while density was varied by almost a factor of three; all other operating parameters, such as plasma current, reversal and parameters were held approximately constant (changed less than 10%). Since a general change in potential occurred that crudely mimics temperature changes, a detailed study of temperature and potential is indicated. In addition to the general decline in potential with increasing density, a pattern of an increase followed by a decrease in potential during the period between sawteeth was also apparent. To compare the potentials observed in different discharges it appears best to synchronize the time dependence to the sawtooth onset times. Studies of this type are underway.

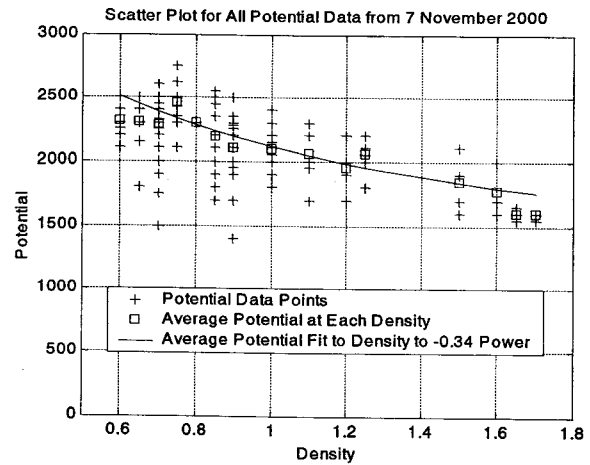


Fig. 4 A scatter plot of all potential data taken at $r/a = 0.5$ during a 50 shot density scan. Density units are normalized to 10^{13} cm^{-3} . Shown are all data points, the average potential at each density, the highest confidence potential data points and a curve fit to the average potential. A systematic error in the detector calibration could require that all voltages shown be reduced by as much as 900 V.

5. Conclusions and Future Directions

HIBP data has also been obtained for many other discharges with quite different conditions (even though only a small fraction of possible MST operating space has been considered). These data have shown very large fluctuation levels, so a study addressing electrostatic fluctuation induced particle transport is proceeding. A very interesting result was obtained in a 380kA discharge when fluctuations above 10kHz were filtered out. The resulting potential looked very much like the measured rotation velocity of an $m = 1, n = 6$ mode. The similarity occurs during and between sawteeth. However, as noted above, the large UV burst during the sawtooth makes any potential data obtained during that time very suspect. Techniques are presently under development to improve potential measurements during and near sawtooth times based on the similarity of the noise signals seen on the four detector plates. It should then be possible to determine if the potential changes immediately with the crash or changes more slowly on the time scale of the relaxation. An interesting comparison case will be nonreversed plasmas ($F_{RFP} > 0$) in which there still are sawtooth crashes, but nearly no change in the rotation speed. During the periods between sawteeth, the UV loading is typically still substantial ($\sim 5 \text{ nA}$). However, it is possible to identify

the UV contribution to the detected signal (using signals from detector plates that collect no ion beam current) and nearly eliminate it.

If RFP transport is dominated by parallel electron motion along stochastic magnetic field lines, then the electrons leave rapidly and set up the radial ambipolar electric field. This is parallel transport, just like in a mirror (but slower since the field line length is longer) and potential should scale with temperature, as it appeared to in the simple experiment described above. This suggests looking at the scaling during improved confinement plasmas where the stochasticity and transport are reduced.

References

- [1] T.P. Crowley, IEEE Trans. Plasma Sci. **22**, 291 (1994).
- [2] U. Shah, K.A. Connor, J. Lei, P.M. Schoch, T.P. Crowley and J. Schatz, Rev. Sci. Instrum. **70**, 963 (1999).
- [3] J. Lei, U. Shah, D.R. Demers, K.A. Connor and P.M. Schoch, Rev. Sci. Instrum. **72**, 564 (2001).
- [4] L. Solensten and K.A. Connor, Rev. Sci. Instrum. **58**, 517 (1987).
- [5] D.R. Demers, U. Shah, J. Lei and K.A. Connor, Rev. Sci. Instrum. **72**, 568 (2001).